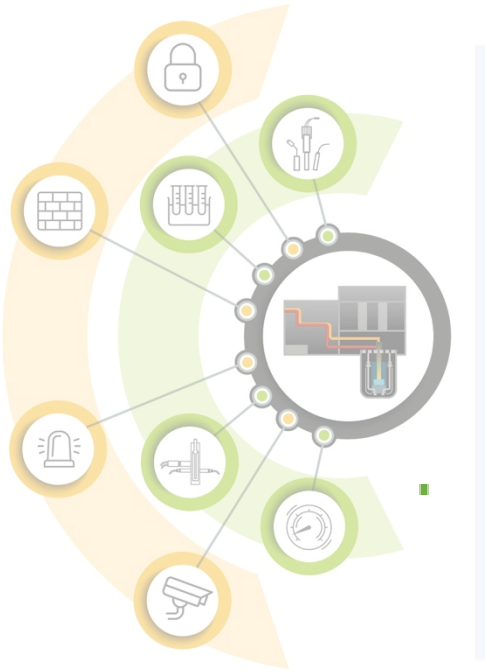

NDA of TRISO Fuels

FY23 Report

Prepared for
US Department of Energy

Mark Croce, Daniel McNeel, Katherine Schreiber, Rico Schoenemann[1]
Jianwei Hu, Callie Goetz, Jason Harp, Wade Ivey, Tammy Keever, Lisa Duncan, Haley Wightman[2]
Daniel Becker[3]
Ammon Williams, Brian Bucher, Edward Seabury, Maegan Coleman, Brian Storms[4]

[1]Los Alamos National Laboratory
[2]Oak Ridge National Laboratory
[3]University of Colorado
[4]Idaho National Laboratory

October 31, 2023
LA-UR-23-32266

SUMMARY

The goal of this measurement campaign is to provide a direct evaluation of nondestructive composition analysis performance between traditional and advanced gamma spectroscopy technologies for irradiated TRISO materials. This work is part of a strategy to enable cost-effective material accounting and safeguards for pebble bed reactors by making use of nondestructive analysis technologies where possible to reduce reliance on sampling and destructive laboratory analysis. Irradiated TRISO compacts, sub-samples of compacts, and dissolved TRISO fuel were measured using high-purity germanium and microcalorimeter detectors at the Oak Ridge National Laboratory Radioactive Materials Analytical Laboratory and Irradiated Fuel Examination Laboratory. Planning was completed for additional measurements at Idaho National Laboratory.

The primary conclusions of this work are:

- The Pu/U ratio of irradiated solid-form TRISO is quantifiable in ultra-high-resolution microcalorimeter spectra using fluoresced Pu and U K X-rays. This ratio is an important safeguards signature and is strongly correlated with burnup.
- The Cs-134/137 ratio measured with HPGe detectors can be used to estimate burnup. Knowledge of the irradiation timeline is needed for this method.
- High-purity germanium and microcalorimeter detectors are complementary in that they each provide the best available energy resolution in the high and low energy regions respectively.

1. INTRODUCTION

Nondestructive analysis technologies are an essential component of existing safeguards frameworks due to their cost-effective and rapid results compared to sampling and destructive laboratory analysis. It is expected that safeguards for advanced reactors such as pebble bed reactors will also benefit from nondestructive measurements at strategic locations. Due to the different nature of pebble bed reactors, TRISO fuels, and the high burnup they can achieve, performance of available measurement technologies must be evaluated for this application. The goal of this measurement campaign is to directly compare nondestructive composition analysis performance between high-purity germanium and microcalorimeter gamma spectrometers for irradiated TRISO fuels. A series of TRISO compacts and sub-samples of compacts from the AGR2 and AGR5/6/7 irradiations were measured at the Oak Ridge National Laboratory Irradiated Fuel Examination Laboratory hot cells. Dissolved fuel materials from AGR2 and AGR5/6/7 were measured at ORNL's Radioactive Materials Analytical Laboratory.

2. MEASUREMENT METHODS

Experience with gamma spectroscopy measurements of dissolved light water reactor fuels [1] led this work to focus on collecting high-statistics spectra with high-purity germanium and microcalorimeter detectors. The gamma ray signatures of AGR2 and AGR5/6/7 were found to be below 1.2 MeV. The Canberra GL1015 low-energy germanium detector was selected due to its good energy resolution, reasonable detection efficiency in the required energy range, and option for electrical cooling which simplified measurement logistics. The GL1015 uses a 15 mm thick, 1000 mm^2 germanium crystal and a 0.5 mm thick Be window with specified resolution of 620 eV FWHM at 122 keV [2]. The SOFIA microcalorimeter spectrometer [3] consists of a multiplexed 256-pixel superconducting transition-edge sensor array in a compact cryostat with aluminum windows. Each of the 256 sensor elements is approximately 1.4 x 1.4 x 0.4 mm thick. The instrument provides energy resolution as good as 60 eV FWHM at 129 keV. The compact adiabatic demagnetization refrigerator cryostat is cooled by a helium pulse tube with air-cooled, single-phase 220 V compressor. SOFIA was used specifically because of its minimal infrastructure requirements and small size, which allowed it to be deployed to the analytical lab and hot cell locations. Larger microcalorimeter instruments that use similar sensors are available with increased detection efficiency including the HERMES-400 instrument at Idaho National Laboratory and the HERMES-700 instrument under development.

This first series of irradiated TRISO measurements focused on identifying signatures of burnup and of fuel composition. Quantitative analysis was based on peak ratios rather than absolute intensities so that measured uncertainty was primarily a function of the material and detector properties rather than the measurement configuration.

3. DISSOLVED TRISO MEASUREMENTS

Dissolved TRISO fuel materials provide a useful comparison to solid form materials to understand matrix effects such as self-attenuation and self-induced X-ray fluorescence. The high burnup of AGR2 and AGR5/6/7 fuels also provides a surrogate for what may be observed from liquid-fueled molten salt reactors. Samples (Table 1) consisted of materials from AGR2 compact 642 and AGR5/6/7 compact 232 dissolved in nitric acid and packaged in plastic or glass vials (Figure 1). The AGR2 samples were initially prepared for destructive analysis of burnup, which determined average burnup values of 10.3 % FIMA. This value differs from the calculated burnup value of 9.26 % FIMA as reported in [4-8]. Calculated burnup values are reported in Table 1 for comparison because destructive analysis burnup values were not available for the AGR5/6/7 samples. The AGR5/6/7 samples were not intended for burnup analysis and do not correspond to complete dissolution of the fuel. While their composition may not be representative of the bulk compact, the samples were observed to contain major components of the fuel.

Sample ID	Related Compact ID	Description	Initial Enrichment $\%^{235}U$	Calculated Burnup %FIMA	Irradiation Dates
AGR2-642-A-S1	AGR2 6-4-2	Burnup sample first extraction analysis aliquot	14.029	9.26	6/22/10-10/16/13
AGR2-642-A-S2	AGR2 6-4-2	Burnup sample second extraction analysis aliquot	14.029	9.26	6/22/10-10/16/13
AGR2-642-B-S2	AGR2 6-4-2	Burnup sample second extraction analysis aliquot	14.029	9.26	6/22/10-10/16/13
230293-002	AGR5/6/7 2-3-2	First burn leach CCCTF fuel holder	15.477	14.36	2/16/18-7/22/20
230293-004	AGR5/6/7 2-3-2	Deconsolidation acid	15.477	14.36	2/16/18-7/22/20

Table 1: Summary of measured dissolved TRISO fuel materials in Radioactive Materials Analytical Laboratory

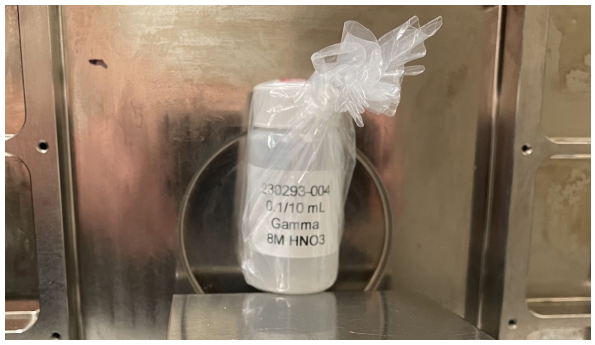

Figure 1: Dissolved AGR2 and AGR5/6/7 materials were packaged in plastic or glass vials for measurement.

4. SOLID FORM TRISO MEASUREMENTS

Solid form TRISO fuels were measured through a collimated port on the East Cell of the ORNL Irradiated Fuel Examination Laboratory. Table 2 summarizes the items measured. Two intact compacts were available: AGR2 compact 211 and AGR5 compact 223. A third item containing about 90% of AGR2 compact 542 was also available. Remaining items consisted of subsamples of compacts. Items were placed at the end of a lead collimator that extended into the hot cell. Detectors were located on a cart (Figure 2) at the other end of the collimator. This configuration allowed the detectors to be easily repositioned to align with the collimator and to adjust count rate when needed. Background was measured with each detector type. Intact compacts were packaged in "dog bone" containers which consist of a section of stainless steel tube with compression fitting end caps (Figure 3). Subsamples of compacts were packaged in aluminum pellet cans.

Due to the gamma dose rate at the detector location a temporary radiation area boundary was established during measurements. Consistent with previous experience, it was found that the multiplexing chips in the SOFIA microcalorimeter gamma spectrometer were unstable in this environment. Lead shielding was placed in front of the microcalorimeter spectrometer, with a hole for the detector window, to reduce dose rate at the multiplexing chips. This configuration effectively eliminated dose effects during measurements of the TRISO materials. X-rays from the shielding did not create additional spectral interferences.

Series	ID	Estimated Particles	Calculated Burnup GWd/MTU	Calculated Burnup %FIMA	Type	Irradiation Dates
AGR2	643A	235	69.7	7.26	UCO	6/22/10-10/16/13
AGR2	642-03	200	93	9.69	UCO	6/22/10-10/16/13
AGR2	621A	235	97.5	10.16	UCO	6/22/10-10/16/13
AGR2	622A	235	97.8	10.19	UCO	6/22/10-10/16/13
AGR2	331-03	150	99	10.31	UO2	6/22/10-10/16/13
AGR2	2-311A	150	101.8	10.6	UO2	6/22/10-10/16/13
AGR2	2-312A	150	102.3	10.66	UO2	6/22/10-10/16/13
AGR2	2-332-03	150	103.5	10.78	UO2	6/22/10-10/16/13
AGR2	2-542	2858	115.5	12.03	UCO	6/22/10-10/16/13
AGR2	2-521A	235	117.9	12.28	UCO	6/22/10-10/16/13
AGR2	212A	235	121.2	12.62	UCO	6/22/10-10/16/13
AGR2	2-222-03	200	121.8	12.69	UCO	6/22/10-10/16/13
AGR2	2-211	3176	120	12.5	UCO	6/22/10-10/16/13
AGR5/6/7	5-222A	235	134.6	14.02	UCO	2/16/18-7/22/20
AGR5/6/7	5-224A	235	137.6	14.33	UCO	2/16/18-7/22/20
AGR5/6/7	5-159A	235	89.2	9.29	UCO	2/16/18-7/22/20
AGR5/6/7	5-413A	235	135	14.06	UCO	2/16/18-7/22/20
AGR5/6/7	5-223	3176	137.6	14.33	UCO	2/16/18-7/22/20

Table 2: Summary of measured TRISO fuel materials at Irradiated Fuel Examination Laboratory hot cells.

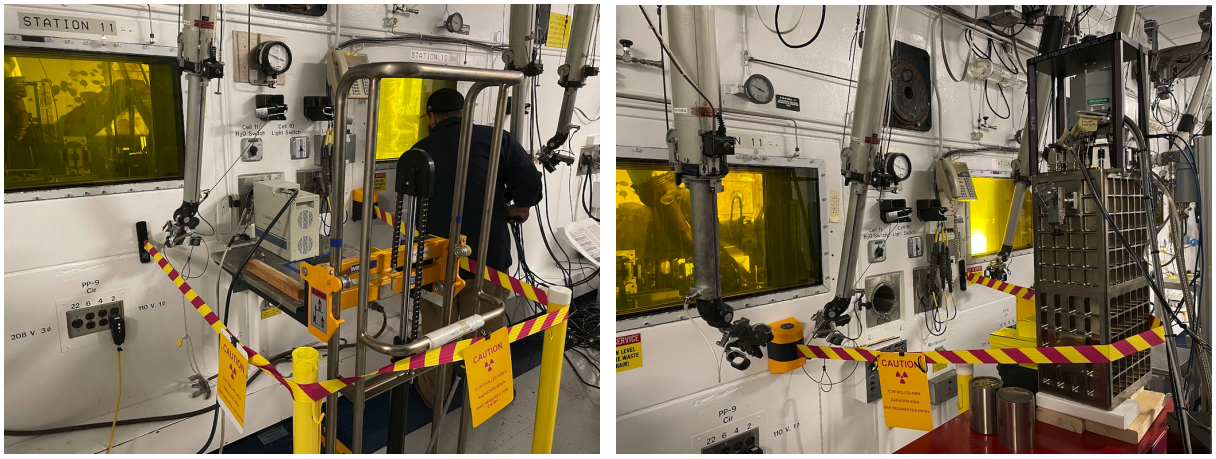

Figure 2: HPGe (left) and microcalorimeter (right) detectors were positioned on a cart in front of the East Cell port. The distance between the detector and port was varied to adjust count rates. Temporary radiation areas were established around the detector due to the gamma dose rate.

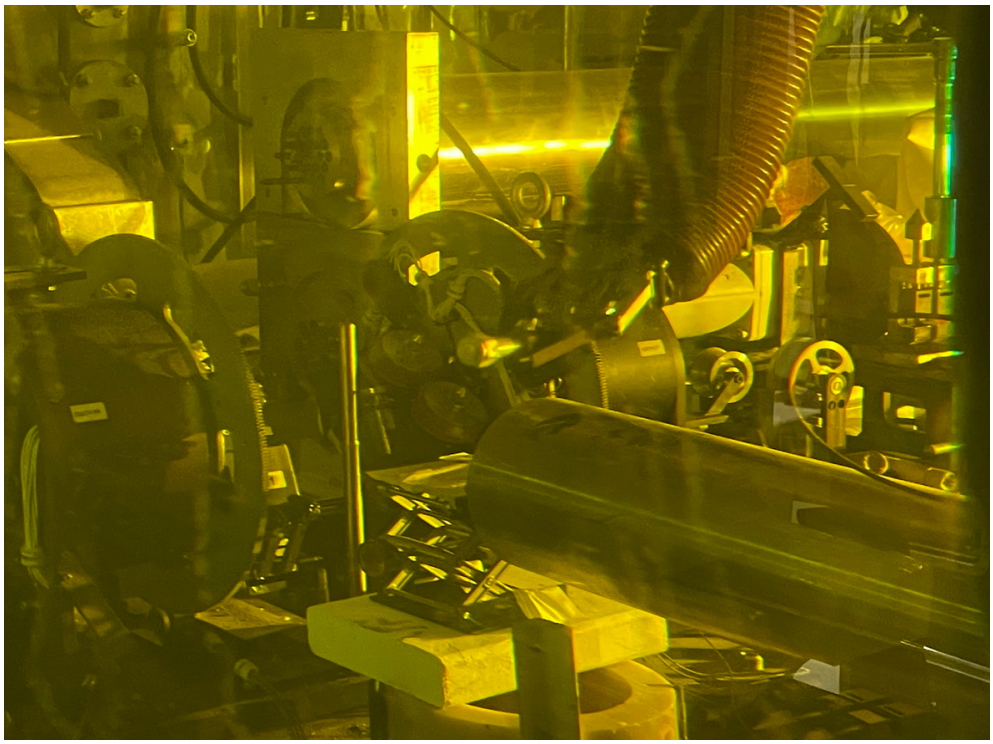

Figure 3: Compacts and subsamples were placed on a stand at the end of the East Cell port collimator. Here, an intact compact packaged in a "dog bone" container consisting of compression fittings on a stainless steel tube, is held in the manipulator.

5. ANALYSIS AND RESULTS

Indicators of burnup and fissile material content were the primary focus of analysis. A major conclusion from prior measurements of dissolved light water reactor fuels is that complementary information is available from HPGe and microcalorimeter spectrometers [1]. This was also observed for dissolved and solid-form TRISO fuels (Figure 4). HPGe provides much better efficiency at energies above approximately 200 keV, with sufficient energy resolution to quantify ratios such as Cs-134 (604 keV) and Cs-137 (662 keV). Microcalorimetry provides additional signatures in the low-energy region (approximately 30-300 keV) where its energy resolution can separate closely spaced peaks. Figure 5A-F shows details of the spectra annotated with primary observations.

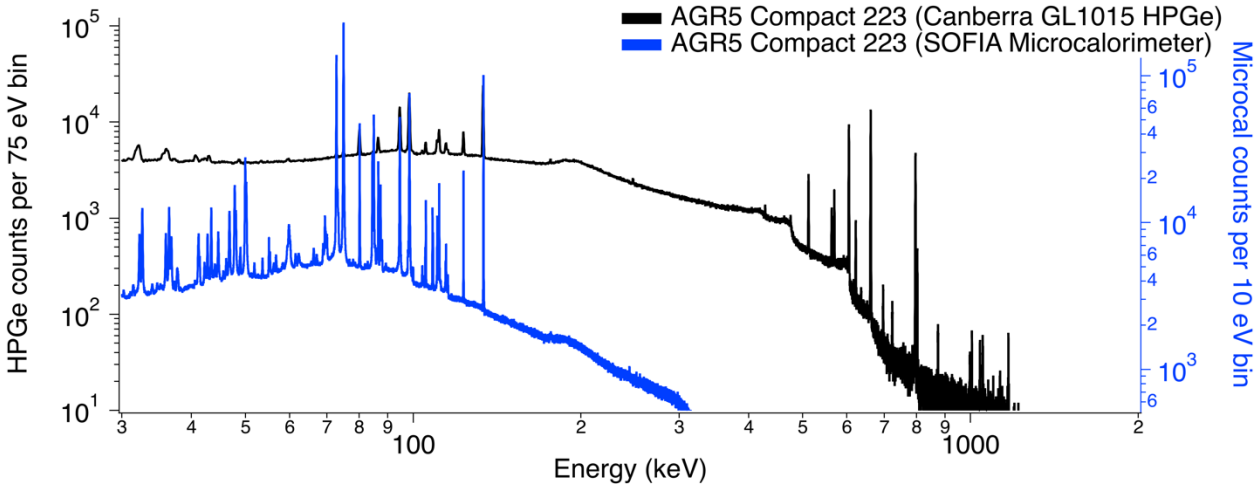

Figure 4: Spectra from intact AGR5 compact 223 measured with both HPGe and microcalorimeter spectrometers show the complementary nature of both technologies, where HPGe efficiency is needed to measure peaks above ~300 keV and microcalorimeter energy resolution is needed to measure closely spaced peaks in the low-energy region.

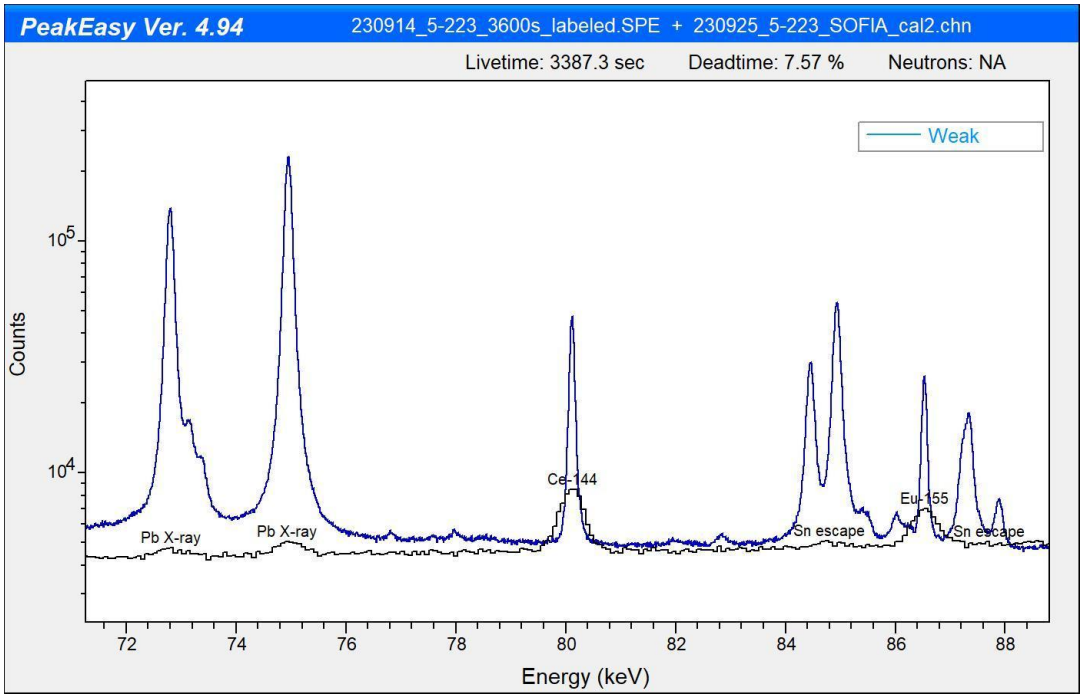

Figure 5A: Region near 80 keV shows lead X-rays from the collimator and shielding, Ce-144, and Eu-155. HPGe data is in black and microcalorimeter data is in blue. Tin X-ray escape peaks are observed in the microcalorimeter data as a result of the tin absorbers in the detector array; however, the tin escape peaks do not appear to interfere with gamma ray peaks in this region.

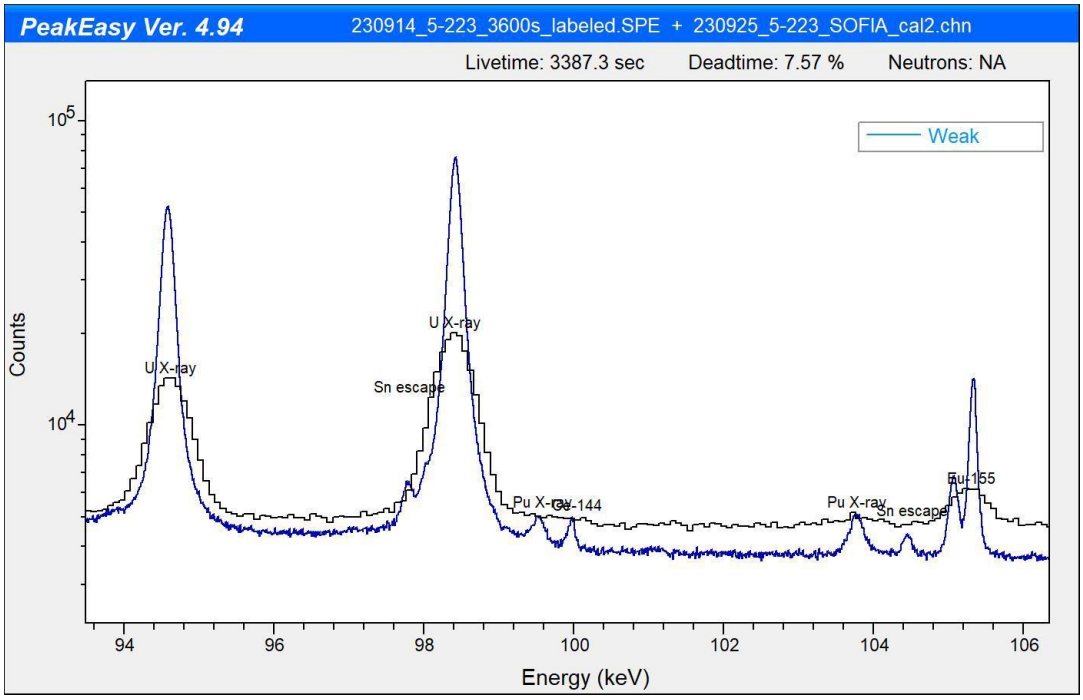

Figure 5B: Region near 100 keV shows U and Pu X-rays from fluorescence, Ce-144, and Eu-155. Microcalorimeter data in blue clearly resolves the Pu X-rays compared to HPGe data in black, which enables direct measurement of the Pu/U element ratio in the fuel from their X-ray peak ratios.

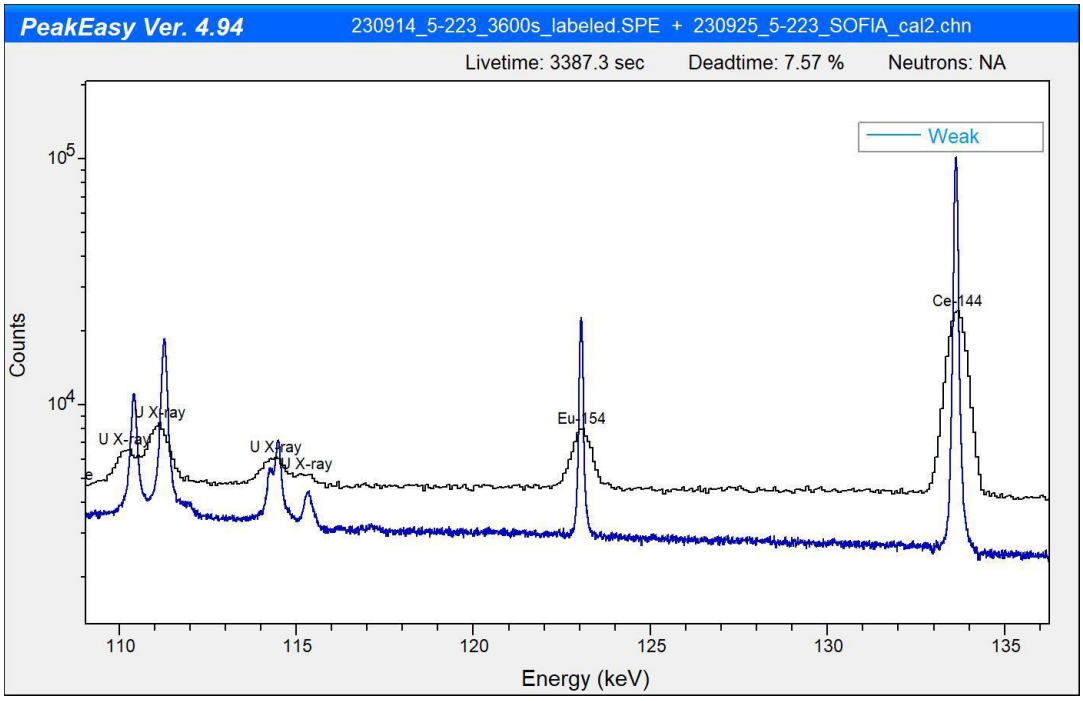

Figure 5C: Region near 120 keV shows U X-rays from fluorescence, Eu-154, and Ce-144. Microcalorimeter (blue) and HPGe (black) provide similar information in this region.

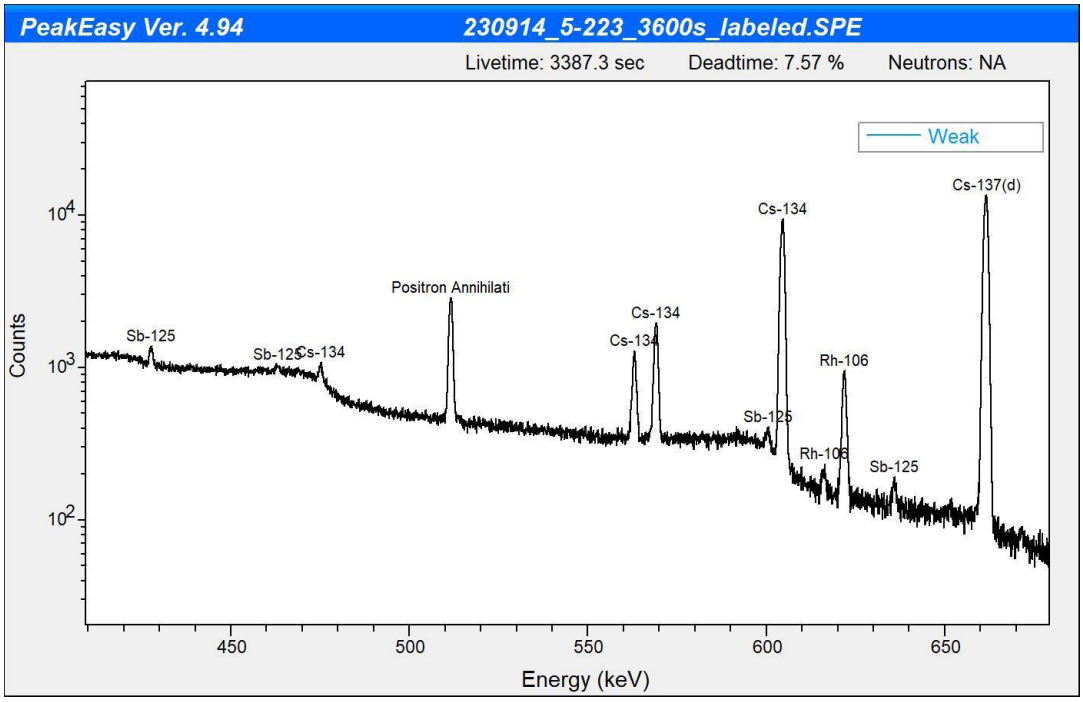

Figure 5D: Region from 400-675 keV shows Sb-125, Cs-134, 511 keV positron annihilation peak from β+ decay and pair production, Rh-106, and Cs-137 in the HPGe spectrum.

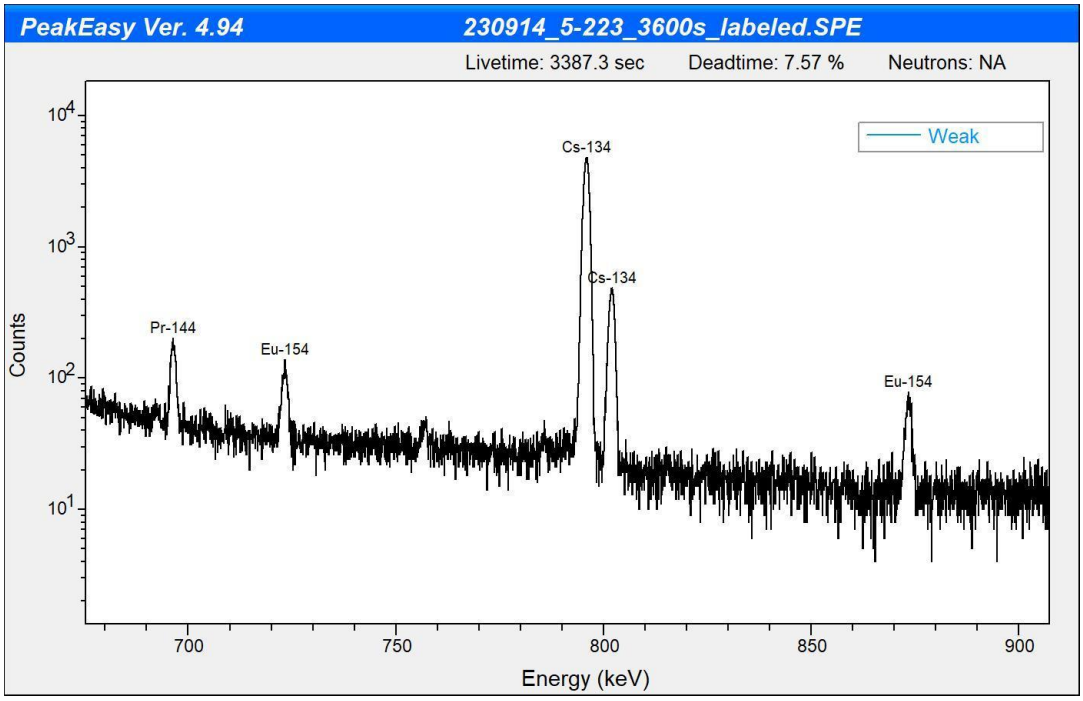

Figure 5E: Region from 675-900 keV shows Pr-144, Eu-154, and Cs-134 in the HPGe spectrum.

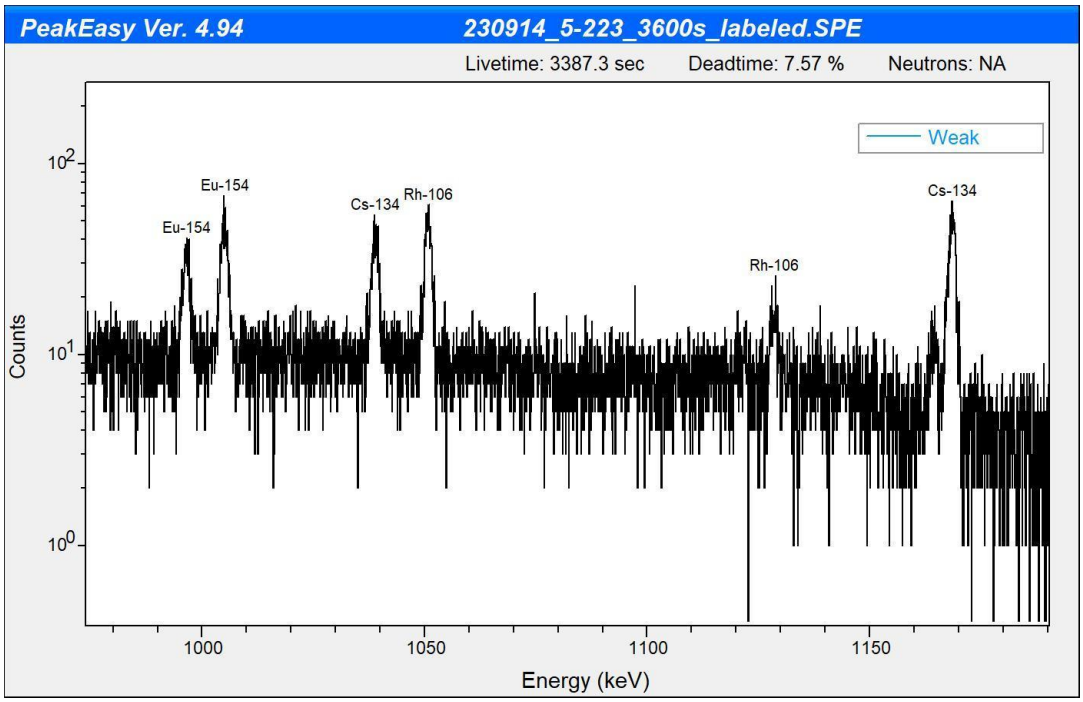

Figure 5F: Region from 900-1200 keV shows Eu-154, Cs-134, and Rh-106 in the HPGe spectrum. No major peaks were observed above 1200 keV.

The gamma-ray background (Figure 6) measured at the East Cell port appeared to be dominated by scattering of gamma rays from items throughout the hot cell. Few peaks were observed in the background spectra, with most of the counts occurring in a broad scattering continuum that peaked between 100 and 200 keV. For the HPGe measurement of AGR5 compact 223, background contributed 0.5% of net counts at 662 keV.

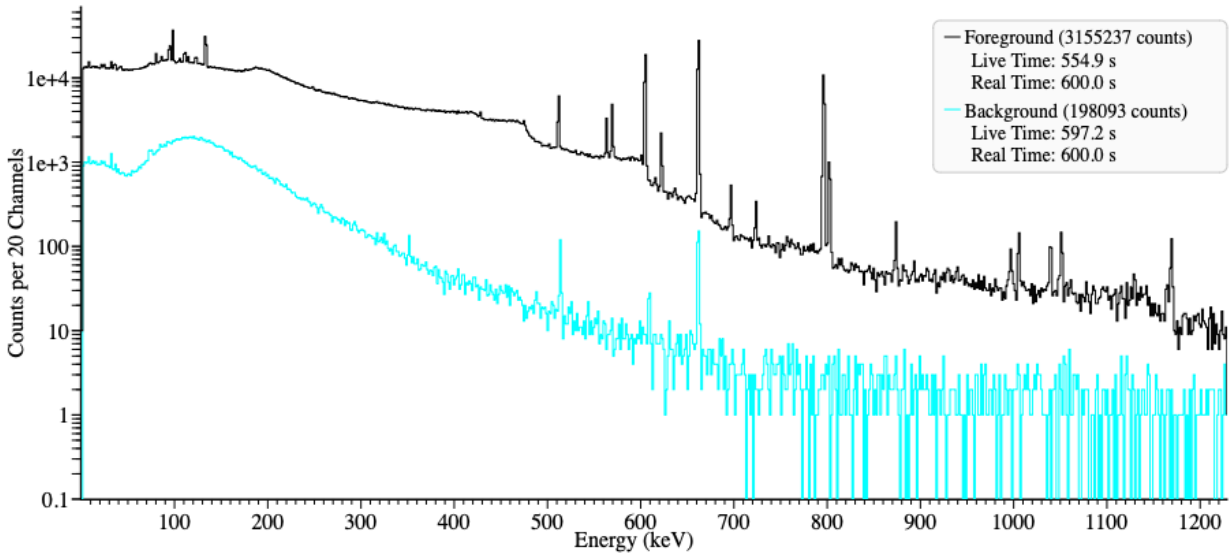

Figure 6: The gamma ray background (blue) was dominated by the scattering continuum with maximum intensity between 100 and 200 keV. For the measurement of AGR5/6/7 compact 223 (black), counts in the 662 keV peak have a 0.5% contribution from background (40114 vs. 218 counts in 600 s)

Fuel burnup estimates using HPGe gamma spectroscopy often use the Cs-134/Cs-137 peak ratio. Cs-134 is a "shielded" fission product that is mainly produced by neutron capture on other fission products, while Cs-137 is directly produced by fission with high yield. Figure 7 shows the results of preliminary peak fits using the Interspec software. For all of the spectra, the measured peak areas did not appear to be a limiting factor in uncertainty. Changing background due to movement of items in the hot cell and incomplete knowledge of the discharge date are likely to be the main factors. There may also be an effect of a different relative efficiency curve between the items due to different packaging or different alignment with the collimator. Further measurements in a lower-background area and with a better-controlled measurement configuration are planned. Due to the short half-life of Cs-134 (2.064 y), this peak ratio is very sensitive to cooling time after discharge. If the reported irradiation dates for AGR2 of 6/22/10-10/16/13 do not apply to all items, for example if the lower-burnup items were removed after fewer irradiation cycles, a correction would need to be applied to interpret the Cs-134 peak area.

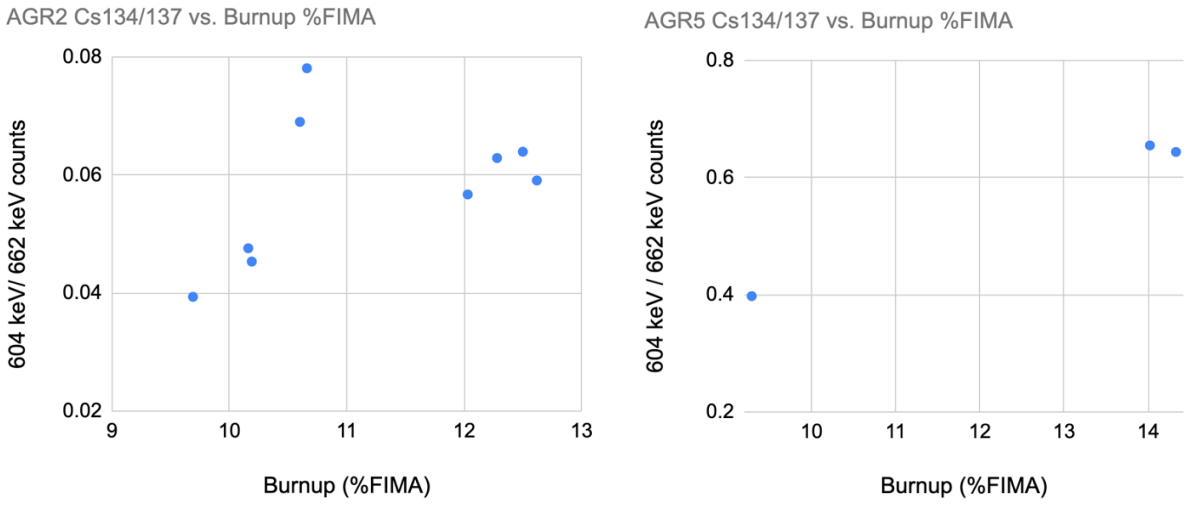

Figure 7: The Cs-134/Cs-137 peak area ratio measured with HPGe is correlated with burnup but also a number of other factors. Limiting factors in uncertainty may include changing background and incomplete knowledge of the irradiation timeline. Further measurements are needed to understand these effects.

In stark contrast to dissolved fuel samples, U and Pu K X-rays were clearly observed in microcalorimeter spectra of solid form TRISO fuel (Figure 8). HPGe spectra were not capable of resolving the Pu X-rays sufficiently for quantitative analysis (Figure 9). These X-rays are understood to result from fluorescence induced by fission product gamma rays. The continuum from scattered gamma rays inside the solid fuel appears to excite U and Pu with similar efficiency, making it possible to use their K X-rays for quantitative analysis of the Pu/U element ratio present within the fuel. In dissolved fuel samples, U and Pu atoms are dispersed at low concentration throughout the liquid matrix and X-ray fluorescence is many orders of magnitude less probable. Previous work has evaluated the potential for self-induced X-ray fluorescence to quantify the Pu/U element ratio in light water reactor fuel rods [9,10]. However, attenuation in conventional fuel pellets limits efficient detection of X-rays to the outer region, and burnup and the Pu/U ratio are known to vary across the diameter. This means the technique is limited when attempting to determine bulk properties of a fuel rod. TRISO fuel is a much more favorable geometry for accurately quantifying the bulk Pu/U ratio because the actinide content is contained in particles dispersed throughout a lower-Z matrix.

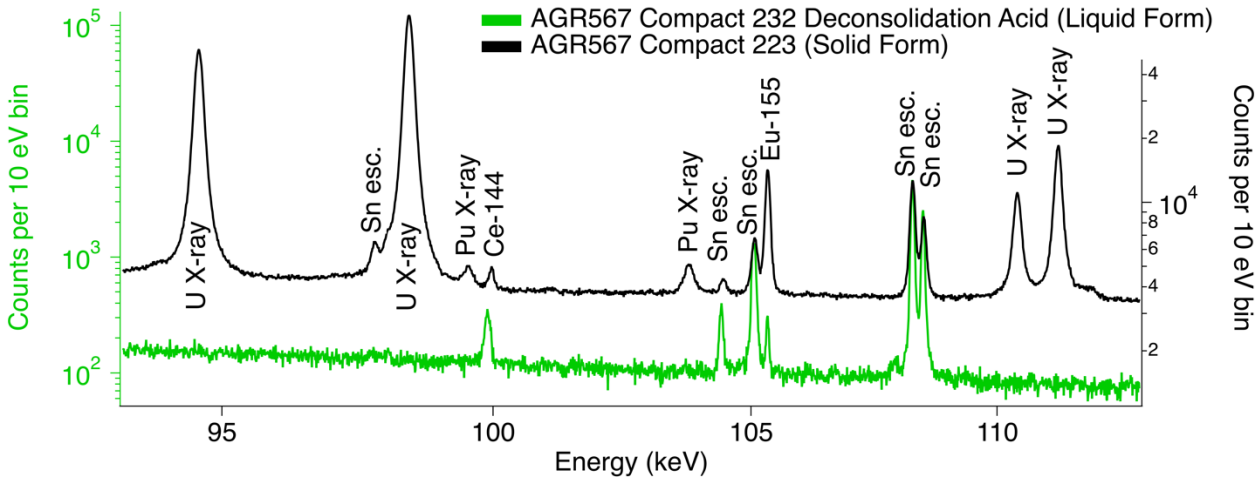

Figure 8: U and Pu fluorescence X-rays are clearly observed in microcalorimeter spectra of solid-form TRISO fuels, in contrast to dissolved fuels. This signature allows the Pu/U element ratio to be directly and nondestructively determined – an important signature for safeguards.

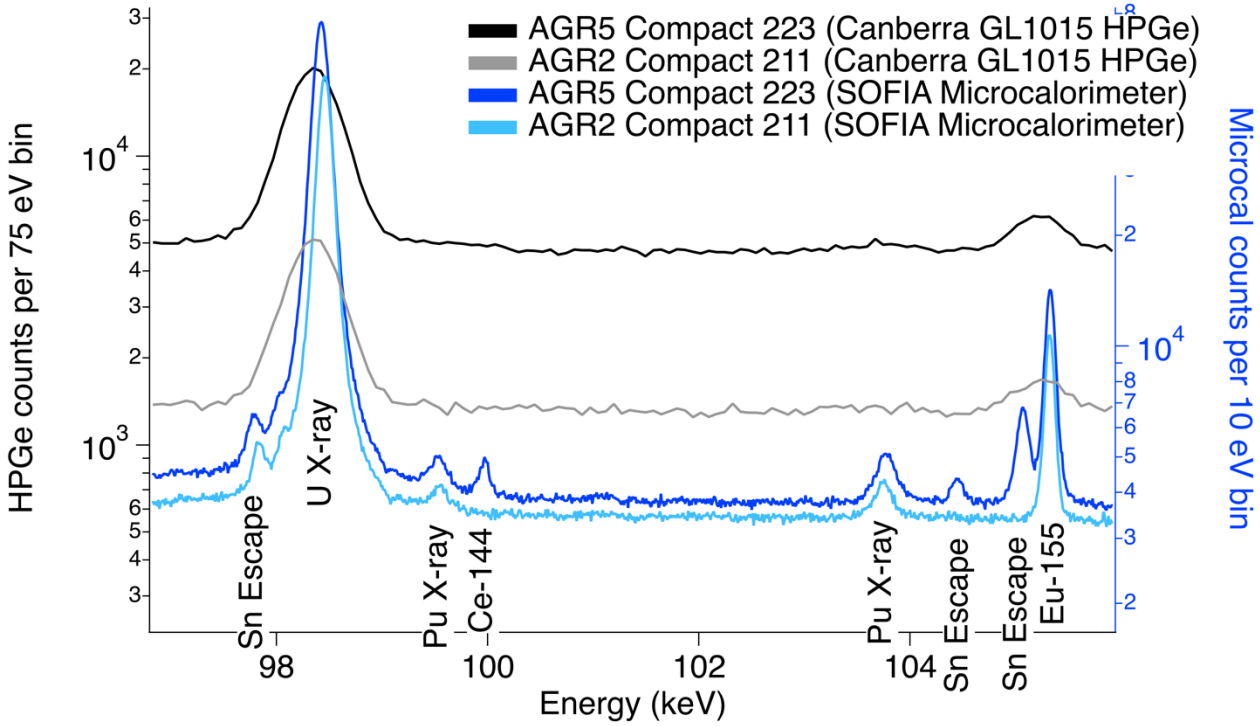

Figure 9: Microcalorimeter data resolves Pu fluorescence X-rays sufficiently for quantitative analysis, while HPGe data does not. Ce-144 is observed only in the more recently-irradiated AGR5 Compact 223, and its gamma rays and associated Sn escape peaks are well-resolved from the U and Pu X-rays.

Accurately inferring a Pu/U ratio from the peak areas of the Ka X-rays of Pu and U is challenging. The best way to make this inference in practice will likely be to measure spectra from a range of materials with known burn-up and Pu/U content, and then build a calibration curve. However, to demonstrate that the measurement results are in the expected range, a simplified first-principles calculation is presented here.

Assuming that the Pu/U content is uniform through the sample the expected peak area for a given peak is:

$$A_{U_{K\alpha 1}} \propto N_U \, X_{U_K} R_{U_{K\alpha 1}} \eta\left(E_{U_{\{K\,\alpha 1\}}}\right)$$

Here A_UKa1 is the area of the U_Ka1 peak, N_U is the number of U atoms present, X_UK is the probability for a K-shell electron to be ejected, R_UKa1 is the probability that the excited atom will relax via the emission of a U_Ka1 X-ray, eta is the total source-detector efficiency curve and E_UKa1 energy of the UKa1 x-ray. Similar expressions apply for the other X-rays. In all cases there are additional constants of proportionality (such as the solid angle subtended by the detector) which are the same for all peaks in a given spectrum.

From this expression the Pu/U ratio follows:

$$\frac{N_{Pu}}{N_U} = \frac{A_{\mathrm{Pu}_{K\alpha 2}}}{A_{\mathrm{U}_{K\alpha 1}}} \frac{X_{\mathrm{U}_K}}{X_{\mathrm{Pu}_K}} \frac{R_{\mathrm{U}_{K\alpha 1}}}{R_{\mathrm{Pu}_{K\alpha 2}}} \frac{\eta\left(E_{\mathrm{U}_{K\alpha 1}}\right)}{\eta\left(E_{Pu_{K\alpha 2}}\right)}$$

The probability X for a K-shell electron to be ejected is the photoelectric effect cross-section. From the XCOM database [11], in the relevant energy range above the K-edge, the cross-section for Pu is 7 % -10 % higher for Pu than for U, but more photons are available to eject U K-shell electrons because U has a lower K-edge. Treating the spectrum observed by the microcal system as a proxy for the field incident on U and Pu atoms, X_UK / X_PuK = 1.10.

The probability for a K-shell vacancy to produce Ka1 and Ka2 X-rays are well known and shown in Table 3 [12].

The total source-detector efficiency curve is difficult to estimate due to the complexity of the source-detector geometry. Because the UKa1 and PuKa2 lines are only 1.1 keV, the efficiency is expected to be nearly the same for each peak. The relative areas of the U Ka lines in each spectrum can be used to check this; any difference from the tabulated ratio R_UKa2 / R_UKa1 should be attributable to a difference in the efficiency curve for the two lines. In all three samples these ratios are within 4 % of the expected value, implying that the difference in efficiency between the UKa1 and PuKa2 lines is about 1 %, which is subdominant to all other sources of efficiency, and thus is ignored here.

Final results for the inferred number ratio of Pu to U are shown in Table 4 for three TRISO items. Calculated ratios are estimates based on fuel burnup modeling. These results suggest that the Pu/U ratio may be directly determined in TRISO pebbles using nondestructive gamma spectroscopy. This is an extremely important parameter for safeguards as it is a direct measure of the fissile material content of the fuel.

Element	Line	TPIV
U	Ka1	0.4628
U	Ka2	0.2893
Pu	Ka1	0.4606
Pu	Ka2	0.2910

Table 3: R-factors for U and Pu K-lines

Item	A_PuKa2	A_UKa1	Measured N_Pu / N_U (%)	Calculated N_Pu/N_pu (%)
5-223	26018 +/- 3.0 %	1899621 +/- 0.1 %	2.40 +/- 0.07	2.53
2-542	4726 +/- 10.9 %	566795 +/- 0.2 %	1.46 +/- 0.16	not available
2-211	13671 +/- 3.1 %	1218543 +/- 0.2 %	1.96 +/- 0.10	1.732

Table 4: Measured Peak Areas and Inferred Pu/U ratios

6. SUMMARY AND NEXT STEPS

The primary conclusions of this work are:

- The Pu/U ratio of irradiated solid-form TRISO is quantifiable in ultra-high-resolution microcalorimeter spectra using fluoresced Pu and U K X-rays. This ratio is an important safeguards signature and is strongly correlated with burnup.
- The Cs-134/137 ratio measured with HPGe detectors can be used to estimate burnup. Knowledge of the irradiation timeline is needed for this method.
- High-purity germanium and microcalorimeter detectors are complementary in that they each provide the best available energy resolution in the high and low energy regions respectively.

Direct measurements at the ORNL hot cells provided access to intact solid-form TRISO compacts and were a valuable demonstration of measurement capabilities in a realistic environment. However, changing background conditions and the difficulty of aligning individual items with the collimator introduced uncertainty in quantitative analysis of burnup. Further measurements are planned both at ORNL and INL in lower-background areas with better-controlled measurement geometries. These measurements will be performed on samples containing single or few solid TRISO particles that can be handled outside of a hot cell, and are expected to allow better quantitative analysis.

ACKNOWLEDGEMENTS

This work is funded through the Advanced Reactor Safeguards Program of the Office of Nuclear Energy within the United States Department of Energy. We gratefully acknowledge support of Brian Woody, John Hines, and the team of operators at the ORNL Irradiated Fuel Examination Laboratory.

REFERENCES

1. *Dissolved Fuel Measurement Campaign Report*, LA-UR-22-32380, 2022.
2. Mirion Technologies Low Energy Detector Data Sheet, www.mirion.com
3. Croce et al., *Electrochemical Safeguards Measurement Technology Development at LANL*, Journal of Nuclear Materials Management, 2021.
4. *Determination of Average Burnup in AGR-2 Compacts 3-3-1, 3-3-2, 2-2-2, and 6-4-2*, ORNL/TM/2019/1315, 2019.
5. *AGR-2 Irradiation Test Final As-Run Report*, INL/EXT-14-32277, 2014.
6. *AGR-2 TRISO Fuel Post-Irradiation Examination Final Report*, INL/EXT-21-64279, 2021.
7. *AGR-5/6/7 Fuel Specification*, INL/MIS-11-21423, 2011
8. *AGR 5/6/7 Irradiation Test Final As-Run Report*, INL/EXT-21-64221, 2021.
9. Hoover et al., *Measurement of Plutonium in Spent Nuclear Fuel by Self-Induced X-ray Fluorescence,* Proceedings of the Institute of Nuclear Materials Management Annual Meeting, 2009.
10. Ziock et al., *Non-Destructive Assay of Spent Nuclear Fuel using Gamma-Ray Mirrors as a Narrow Band Pass Filter*, osti.gov, 2023

11. NIST XCOM database, https://www.nist.gov/pml/xcom-photon-cross-sections-database, 2023.
12. Zschornack, *Handbook of X-ray Data*, Springer, 2007.